The Stability, Toxicity, and Reactivity of Zero Valent Iron Nanoparticles

by
Hannah G. Bulovsky

A THESIS

submitted to

Oregon State University

Honors College

in partial fulfillment of
the requirements for the
degree of

Honors Baccalaureate of Science in Chemical Engineering
(Honors Associate)

Presented June 9, 2015
Commencement June 2016

AN ABSTRACT OF THE THESIS OF

Hannah G. Bulovsky for the degree of Honors Baccalaureate of Science in Chemical Engineering presented on June 9, 2015. Title: The Stability, Toxicity, and Reactivity of Zero Valent Iron Nanoparticles.

Abstract approved:_____

Stacey L. Harper

Zero valent iron nanoparticles effectively remediate groundwater contaminants due to their catalytic properties and enhanced surface area. However, these properties contribute to particle agglomeration, decreasing their effectiveness. In this study, we examined the effect of two stabilizing agents (gum arabic (GA) and sodium carboxymethyl cellulose (CMC)) on particle stability, toxicity, and reactivity. Stability was assessed by measuring particle hydrodynamic diameter (HDD). The HDD of the unstabilized particles was over 1000 nm, while the CMC and GA stabilized particles were around 200 nm. Embryonic zebrafish were used to investigate the sublethal toxicity and mortality resulting from particle solution exposure over 5 days. The CMC stabilized particles and unstabilized particles caused significant mortality at lower concentrations, while lower concentrations of GA stabilized particles only caused hatching delay. Reduction of trichloroethylene (TCE) was assessed using gas chromatography following a 24 hour incubation. The concentration of TCE only decreased when incubated with GA and CMC stabilized particles. The small HDD of the particles synthesized with stabilizers indicated these compounds stabilized the particles. GA stabilized particles had the smallest HDD, led to the greatest decrease in TCE, and were assessed to be the least toxic in this study.

Key Words: Zero valent iron, nanoparticles, zebrafish, trichloroethylene

Corresponding e-mail address: hgbulovsky@gmail.com

The Stability, Toxicity, and Reactivity of Zero Valent Iron Nanoparticles

by
Hannah G. Bulovsky

A THESIS

submitted to

Oregon State University

Honors College

in partial fulfillment of
the requirements for the
degree of

Honors Baccalaureate of Science in Chemical Engineering
(Honors Associate)

Presented June 9, 2015
Commencement June 2016

Honors Baccalaureate of Science in Chemical Engineering project of Hannah G. Bulovsky presented on June 9, 2015.

APPROVED:

Stacey L. Harper, Mentor, representing Chemical, Biological, and Environmental Engineering

---

Jeffrey A. Nason, Committee Member, representing Chemical, Biological, and Environmental Engineering

---

Lewis Semprini, Committee Member, representing Chemical, Biological, and Environmental Engineering

---

Toni Doolen, Dean, Oregon State University Honors College

I understand that my project will become part of the permanent collection of Oregon State University, Honors College. My signature below authorizes release of my project to any reader upon request.

Hannah G. Bulovsky, Author

Acknowledgements

This work was supported by the Pete and Rosalie Johnson Internship Program, the DeLoach work scholarship, the Honors Experience Scholarship, and the Undergraduate Research, Innovation, Scholarship, and Creativity award, the Air Force Research Lab AFRL FA8650-05-1-5041, and the NIH ONES grant ES017552-01A2. The transmission electron microscope (TEM) images are based upon work supported by the National Science Foundation via the Major Research Instrumentation (MRI) Program under Grant No. 1040588. We also gratefully acknowledge financial support for the acquisition of the TEM instrument from the Murdock Charitable Trust and the Oregon Nanosciences and Microtechnologies Institute (ONAMI). The author would like to acknowledge the research team in Dr. Stacey Harper's Nanotoxicology Laboratory and the laboratory manager Bryan Harper, Teresa Sawyer and Peter Eschbach for their assistance with the TEM, Dr. Lewis Semprini and Dr. Mohammed Azizian for providing access to gas chromatograph instruments and assisting with their use. The author would also like to thank Pete and Rosalie Johnson, the School of Chemical, Biological, and Environmental Engineering at Oregon State University, Dr. Skip Rochefort for their support of this work.

Contents

Chapter 1 – General Introduction

Groundwater is used in homes, agriculture, industry, and sometimes serves as a drinking source for wildlife worldwide. Brought to the surface either mechanically or naturally, contaminated groundwater poses a threat to both animal and human health (Yang and Rauckman, 1987). Traditional remediation techniques such as site containment and pump-and-treat are costly, time consuming, and frequently ineffective (Cundy et al., 2008). Zero valent iron filings have been implemented successfully at several sites as a permeable reactive barrier through which the contaminated plume flows (Bilardi et al., 2013), but implementing these barriers disturbs the soil which can be costly, and these barriers can become clogged and ineffective over time.

Zero valent iron nanoparticles (nZVI), particles with at least one dimension under 100 nanometers, have been found to be more effective than their non-nano counterparts for remediation due to their high surface area to volume ratio and increased mobility in contaminated target zones (He, 2007). It has been shown that chlorinated compounds, pesticides, certain heavy metals, and other pollutants are converted into less hazardous forms via sequestration, transformation, or degradation by zero valent iron. The increased surface area of the nanoparticles provides more reactive sites on each particle which increases the rate and reaction capacity of the zero valent iron solution (O'Carrol, 2012).

The highly reactive and magnetic properties of nZVI cause them to rapidly agglomerate, which reduces the mobility of the particles in soil and diminishes their reactivity. To overcome the attractive forces between the particles, stabilizing compounds can be added to the particle solution during synthesis (O'Carrol, 2012). Stabilizers commonly employ electrostatic and steric hindrance to keep the particles small and

suspended in solution. Electrostatic hindrance works by creating a charged layer around each particle, overcoming the attractive forces that draw the particles together and causing them to actively repel each other. Compounds that provide steric stabilization create a protective layer between the particles that works to counteract their attractive forces by creating distance between the particles (Sakulchaicharoen, 2010). An example of steric and electrostatic stabilization is shown in Figure 1.

Steric Stabilization Electrostatic Stabilization

Figure 1: In sterically stabilized particle dispersions large polymers block particles from getting close enough for the attractive forces to cause them to agglomerate, while electrostatic stabilization keeps particles from agglomerating by coating each particle with like-charged polymers which repel each other.

The most effective stabilizers are found to be high molecular weight anionic polyelectrolytes that provide both electrostatic and steric stabilization to the particle suspension (O'Carrol, 2012).

Dynamic light scattering (DLS) can be used to determine the hydrodynamic diameter (HDD) and size distribution of nanoparticles using laser light. The HDD is measured as the diameter of a particle or in some cases, the agglomerates, including the layer of hydration surrounding the particle. A laser is shown through a cuvette containing the nanoparticle sample. The Brownian motion (random particle motion due to collisions with other particles and molecules) of the particles causes the laser light to be reflected at different intensities. The reflected light can be correlated to the Brownian motion of the

particles, and the Brownian motion of the particles is related to the size of the particles through the Stokes-Einstein Relationship shown in Equation 1 (Malvern).

$$D_H = \frac{k_B T}{3\pi\eta D_t} \quad (1)$$

D_H is the HDD of the particles, k_B is Boltzman's constant, T is the temperature of the sample, η is the viscosity of the sample, and D_t is the diffusion coefficient of the particles determined by DLS.

Nanoparticle Tracking Analysis (NTA) is another method used to determine the size of nanoparticles. NTA works similarly to DLS; a laser light is shown through the sample and the light is scattered by the Brownian motion of the particles. The scattered light is captured by a microscope connected to a video camera. This allows a video file of the movement of the particles to be created. This video is then analyzed using NTA software, which tracks and calculates the size of each individual particle using the Stokes-Einstein relation shown in Equation 1. NTA can be used to determine particle size and concentration.

pH is a measure of the acidity or alkalinity of a solution calculated using the concentration of hydrogen ions, $[H^+]$, in a solution. pH can affect the zeta potential (ZP) of the solution, which is a widely used measure of the interactions between the particles. Lower pH solutions can cause a buildup of positive charge on the particles, while solutions with high pH can cause a buildup of negative charge. In a plot of ZP vs. pH for a particle solution, there will be a point where the ZP passes through zero. This is called the isoelectric point, and is the point where the solution is the least stable.

ZP is the potential at the barrier between the bulk liquid and the ionic layer that forms around particles. If all the particles in a solution have large positive or negative ZP values, they will repel other similarly charged particles. The particles then cannot get close enough to bind to each other, which leads to a stable solution. ZP values above 30 mV or below -30 mV are considered to indicate a very stable particle system, while ZP values near zero indicate an unstable solution.

Transmission electron microscopy (TEM) is a microscopy technique that can be used to investigate the morphology of nanoparticles. Particle samples are mounted on grids which are placed in a vacuum chamber within the instrument. A beam of electrons is then passed through the sample, and some electrons are deflected by the sample. An image of the sample is created from the electrons that are not scattered, and in this way nanoparticles can be visualized. Some TEM instruments can perform scanning TEM. This imaging technique also uses a beam of electrons to visualize particles, but instead of passing a continuous beam through the sample the beam scans the particle. Scanning TEM can be used to obtain higher resolution images.

Chapter 2 – Synthesis and Stabilization

2.0 Introduction

nZVI were synthesized in the presence of the stabilizer using a modified version of the synthesis method outlined by He and Zhao (He and Zhao, 2007). Sodium carboxymethyl cellulose (CMC), gum arabic (GA), polyvinylpyrrolidone (PVP), and tannic acid (TA) were investigated as stabilizers, ferrous sulfate functioned as the iron source, and sodium borohydride acted as the reducing agent. CMC has been found to be an effective stabilizer for nZVI and is used frequently, necessitating toxicological investigation. It was also used here as a positive control for stabilization. GA was investigated as a possible stabilizer for nZVI because it is known to prevent agglomeration of silver nanoparticles effectively (Lin *et al.*, 2012).

CMC, GA, and TA are all classified by the FDA as substances that are generally recognized as safe (GRAS) with a conclusions type 2, which says that "there is no evidence in the available information on [substance] that demonstrates a hazard to the public when it is used at levels that are now current and in the manner now practiced. However, it is not possible to determine, without additional data, whether a significant increase in consumption would constitute a dietary hazard," (FDA).

2.1 Materials and Methods

2.1.0 Particle Synthesis (Method 1) and Characterization

The compounds used for stabilization are non-hazardous; GA is used to stabilize food mixtures and soft drinks (Islam *et al.*, 1997), and CMC is used frequently in food

processing applications (He *et al.*, 2007). TA occurs naturally in many foods (FDA), and PVP is used as a binder for oral pharmaceuticals.

CMC from Sigma-Aldrich (CAS 9004-32-4) with an average molecular weight of about 90,000 was used in all CMC nZVI synthesis experiments. GA (CAS 9000-01-5), TA (CAS 1401-55-4), and PVP (CAS 9003-38-9) were also all obtained from Sigma-Aldrich. The method used in this work to synthesize the iron nanoparticles was adapted from the methods used by He and Zhao (He and Zhao, 2007). The stabilizer solution containing 100 mL of Milli-Q water (Millipore, Massachusetts, USA) and 0.8 wt% sodium carboxymethyl cellulose, polyvinylpyrrolidone, gum arabic, or tannic acid, was heated under vacuum until boiling began to remove excess dissolved oxygen. Then the solution was removed from heat and 10 mL of 0.21 M ferrous sulfate heptahydrate was added. Then the solution was placed in an ice bath for 20 minutes prior to the addition of 10 mL of 0.42 M sodium borohydride. The solution was then hand agitated under vacuum for about 15 minutes until the evolution of hydrogen gas ceased. The solution was filtered through a 0.22 μm syringe filter to remove excess stabilizer and the particles were then immediately characterized. A NanoSight NS500 (NanoSight industries, California, USA) was used to determine particle hydrodynamic radius and a ZetaPALS (Brookhaven Instruments Corporation, New York, USA) was used to measure HDD via dynamic light scattering, and the zeta potential of the solution. Student-t tests assuming equal variance were used to determine significant differences between all data.

2.1.1 Particle Synthesis (Method 2) and Characterization

This method was used to synthesize all particles used in toxicity and reactivity tests. It was adapted from the methods used by He and Zhao (He and Zhao, 2007). The stabilizer solution contained 50 mL of Milli-Q water and 0.8 wt% sodium carboxymethyl cellulose or 2.0 wt% gum arabic, was heated to dissolve the stabilizing compound, then placed in an ice bath for 15 minutes. The stabilizer was then added to 50 mL of ferrous sulfate (0.21 M), and the resulting solution was purged with nitrogen for 15 minutes to removed dissolved oxygen on a shaker table at 200 rpm. Then 50 mL of a 0.42 M sodium borohydride solution was prepared and then immediately added to the ferrous sulfate and stabilizer mixture under vacuum over the course of 2 minutes using a 50 mL syringe. Following the addition of sodium borohydride, the solution was shaken at 200 rpm under vacuum for 15 minutes, then immediately characterized for size and ZP using a Malvern Zetasizer (Malvern Instruments, Worcestershire, United Kingdom) and NanoSight NS500. The pH of particle solutions was determined using a sympHony B30PCI pH probe (VWR International). All syntheses were performed in triplicate. Student-t tests assuming equal variance were used to determine significant differences between all data. All graphical error bars represent the standard error of the mean, calculated by dividing the standard deviation between the replicates by the square root of the number of replicates.

All TEM images were obtained using a FEI Titan 80-200 TEM/STEM with ChemiSTEM capability at Oregon State University.

2.2 Results

2.2.0 Synthesis Method 1

Unstabilized and CMC, GA, and PVP stabilized nZVI were synthesized using particle synthesis method 1 described in section 2.1. The particles stabilized in the presence of TA had extremely variable sizes, and agglomerated quickly so these results are not shown. Figure 2 shows the average particle HDD of particles synthesized using particle synthesis method 1.

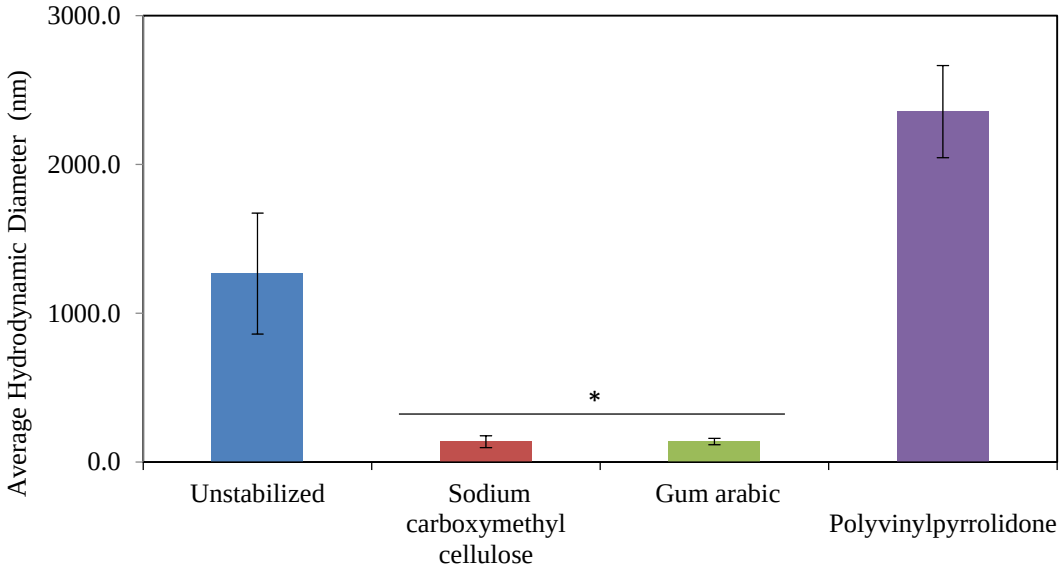

Figure 2: Average HDD of particles synthesized using particle synthesis method 1 measured using DLS with a Brookhaven ZetaPALS instrument with standard error bars. nZVI synthesized in the presence of CMC and GA had significantly smaller HDDs than the PVP and unstabilized nZVI.

Unstabilized nZVI had an average HDD over 1000 nm and particles synthesized with PVP were over 2000 nm, while particles synthesized with CMC and GA were under 200

nm. The particles synthesized with CMC and GA were significantly (* = P < 0.05) smaller than the unstabilized particles and particles synthesized with PVP.

The average HDD of unstabilized particles and particles synthesized with CMC, GA and PVP measured using NTA are shown in Figure 3.

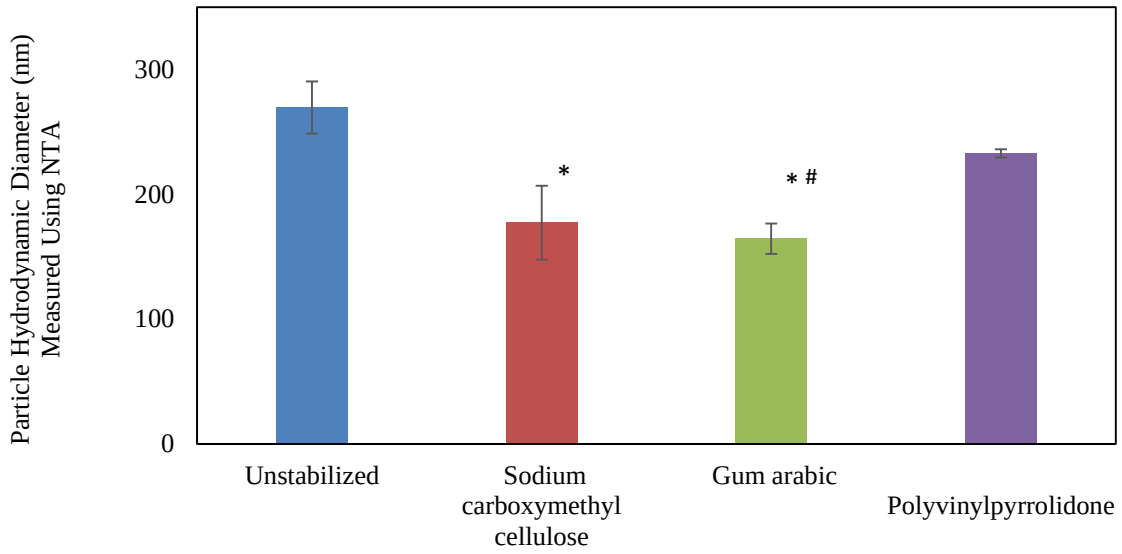

Figure 3: The average HDD of particles measured using NTA. Particles synthesized with CMC and GA were significantly smaller than unstabilized particles. Particles synthesized with GA were significantly (# = P < 0.05) smaller than particles synthesized with PVP.

Particles that were not synthesized without a stabilizing compound were around 270 nm, and particles synthesized with PVP were about 233 nm. Particles synthesized with CMC were about 177 nm, and particles synthesized with GA were 164 nm. Particles synthesized with CMC and GA were significantly smaller than unstabilized particles, and particles synthesized with GA were significantly (# = P < 0.05) smaller than particles synthesized with PVP.

Representative particle distribution curves collected using NTA are shown below in Figure 4.

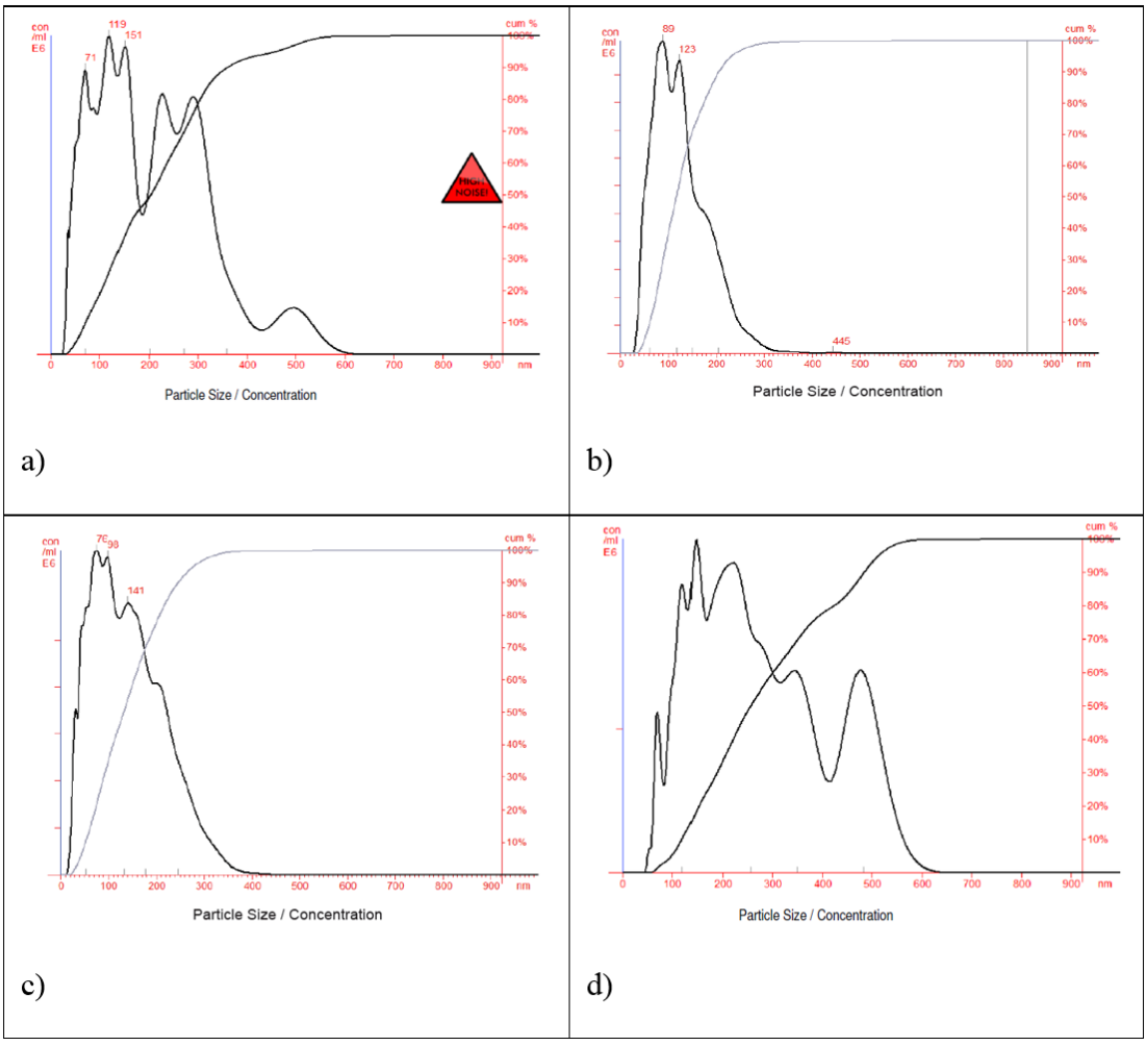

Figure 4: Representative curves showing the particle size distribution for a) unstabilized nZVI, b) nZVI synthesized with CMC, c) and nZVI synthesized with GA, and d) nZVI synthesized with PVP measured using NTA.

The particle size distributions in Figure 4 show the unstabilized particles and those synthesized with PVP have wider particle size distributions than those synthesized with CMC and GA.

The ZP of particles synthesized in the presence of CMC and GA was significantly larger than the ZP of unstabilized particles and particles synthesized in the presence of PVP, as shown in Figure 5.

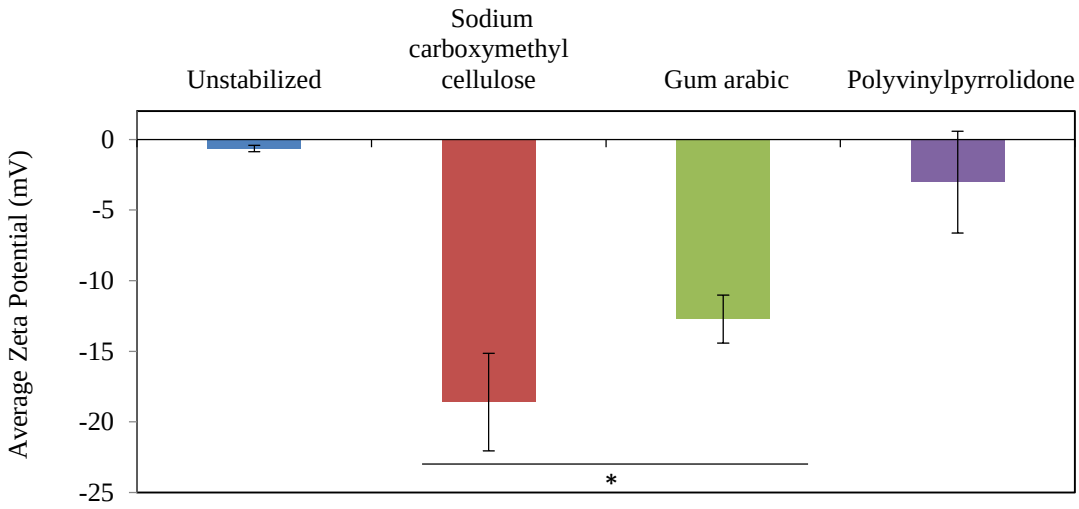

Figure 5: The average ZP of particles synthesized using particle synthesis method 1 with standard error bars. Particles synthesized with CMC and GA had significantly larger ZP values than unstabilized particles and particles synthesized with PVP.

Unstabilized particles and particles synthesized with PVP had average ZP values of -0.63 mV, and -3.0 mV respectively. Particles synthesized with CMC had an average ZP values of -18.6 mV, and the ZP value of GA particles was -12.7 mV.

2.2.1 Synthesis Method 2

Particle synthesis method 1 was modified in an attempt to produce particles that were more uniform and stable. The amount of GA used during particle synthesis was increased from 0.8 to 2.0 wt% in an attempt to increase stabilization. Additionally, the stabilizer and iron solution was purged with nitrogen to remove dissolved oxygen and prevent the oxidation of ferrous sulfate before particle formation. In method 2, the

sodium borohydride was added using a syringe to increase nanoparticle formation, and the solution was shaken on a shaker plate during nitrogen purging and sodium borohydride addition to increase mixing. Particles synthesized in the presence of CMC and GA were smaller and had larger ZP values, so they were chosen for further investigation. PVP did not produce nZVI that were significantly different than unstabilized particles, and the use of TA did not produce consistent nZVI so these materials were not investigated further as stabilizers.

Using synthesis method 2, the average HDD measured using a Malvern DLS instrument of unstabilized particles was over 3000 nm, while particles synthesized with CMC and GA were around 350 nm and 233 nm in diameter respectively. Particle average HDDs are shown in Figure 6.

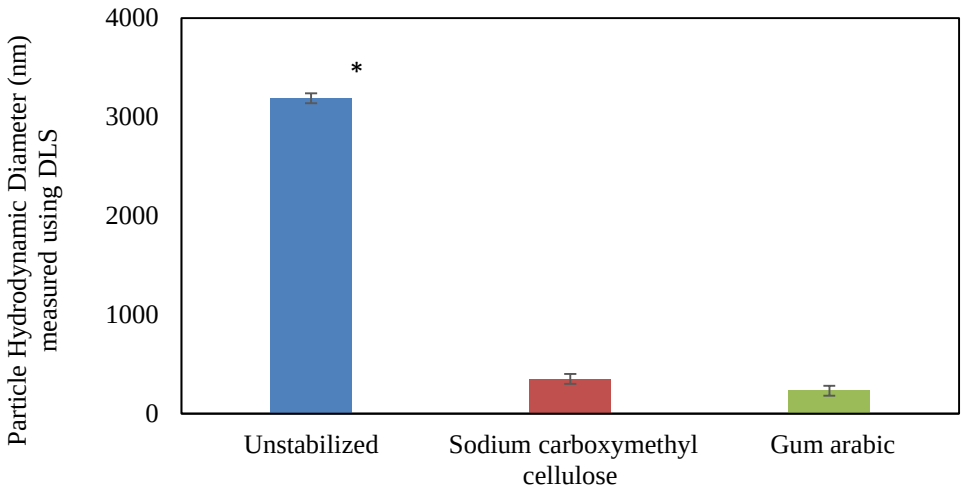

Figure 6: The average HDD of particles synthesized using particle synthesis method 2 with standard error bars. Unstabilized particles were significantly larger than particles synthesized with CMC and GA.

The unstabilized particles were significantly larger than the particles synthesized with CMC and GA. The average particle HDD measured using DLS increased after using particle synthesis method 2.

The size of the particles was also measured using the NanoSight NS500 instrument, and the average particle diameter is shown in Figure 7. Unstabilized particles were around 300 nm, and particles synthesized with CMC and GA were around 183 and 118 nm respectively.

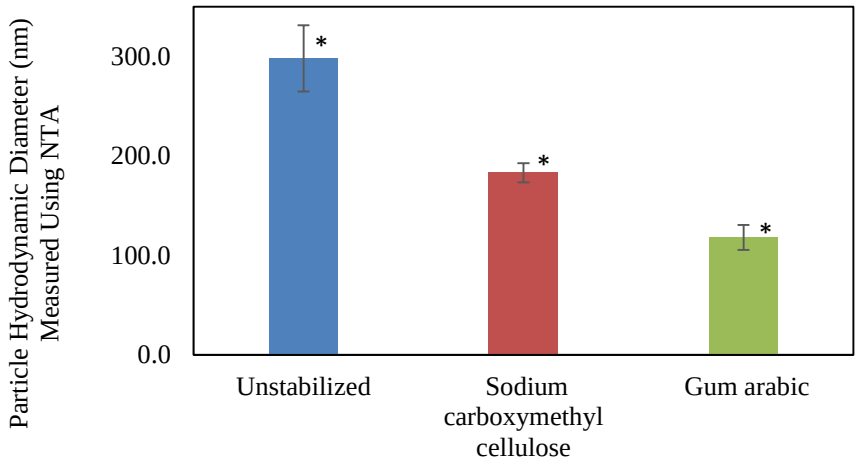

Figure 7: The average HDD of particles synthesized using synthesis method 2 with standard error bars. Each particle diameter was significantly different from the other particle diameters.

The average HDD of each particle solution was significantly different than the other two average particle HDDs when measured using NTA. The unstabilized particles had the largest average HDD, and particles synthesized with GA had the smallest.

The average HDD measured using NTA of particles synthesized using method 1 and method 2 were compared, and are shown in Figure 8.

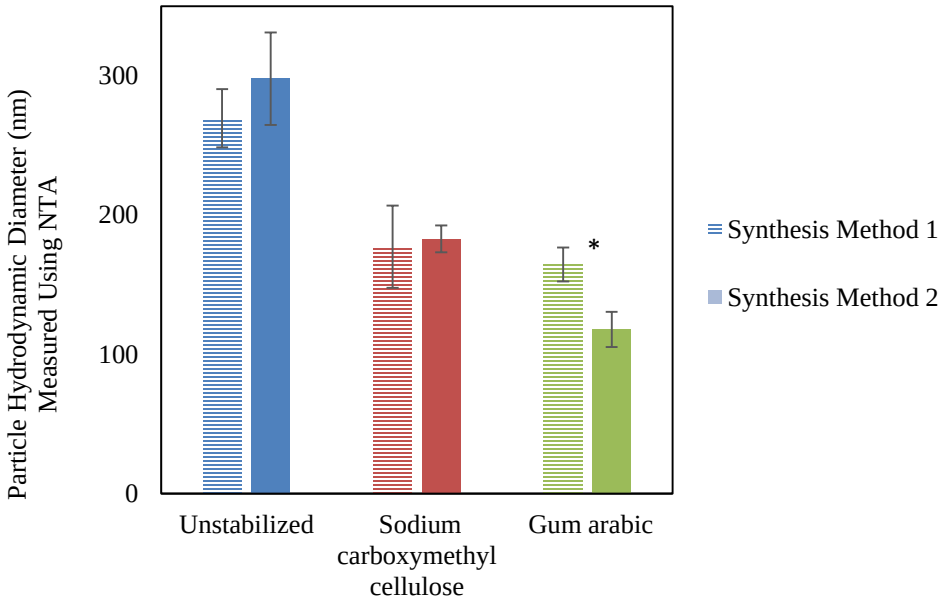

Figure 8: The average HDD of particles synthesized using synthesis method 1 and 2 shown with standard error bars. Significant difference is shown where particle HDD differed between synthesis method 1 and 2.

Particles synthesized with GA were significantly smaller when using synthesis method 2, while unstabilized and particles synthesized with CMC were not significantly different after using synthesis method 2. Additionally, the standard error of particles synthesized with CMC decreased when synthesis method 2 was used. Significant difference in Figure 8 is only shown where the average HDD of particles synthesized with the same compound is different.

The ZP of particles synthesized using method 2 was measured, and the results are shown in Figure 9.

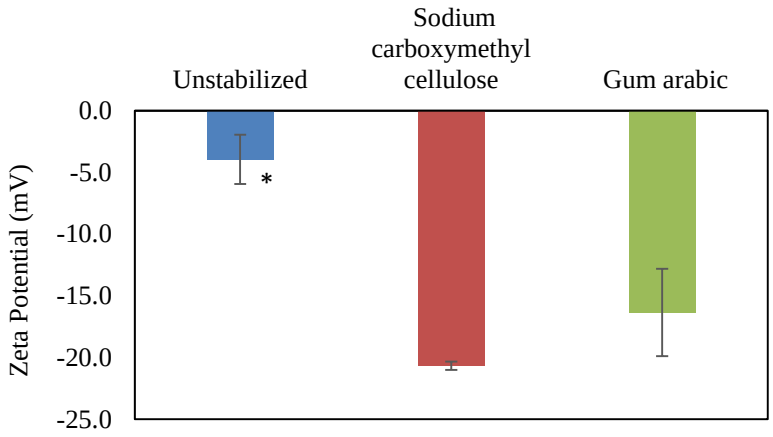

Figure 9: The ZP of particles synthesized using method 2 shown with standard error bars. The ZP of the unstabilized particles was significantly smaller than that of particles synthesized with CMC and GA.

Unstabilized particles had a ZP value of about -4 mV, while particles synthesized with CMC and GA had ZP values of around -21 and -16 mV respectively. Unstabilized particles had a ZP value that was significantly smaller than the ZP value of particles synthesized with CMC and GA. The ZP values of each particle solution were larger when synthesis method 2 was used, but not significantly larger.

The pH of unstabilized particles and particles synthesized with CMC and GA was measured. The results are summarized in Table 1.

Table 1: pH of unstabilized particles and particles synthesized with CMC and GA. There were no significant differences between the three particle solutions.

pH of Particle Solutions	
Particle Solution	**pH**
Unstabilized	5.09
CMC	6.24
GA	5.97

The pH of unstabilized particles was around 5.0, while the solution containing particles synthesized with CMC had a pH of around 6.2 and the solution of particles synthesized with GA had a pH of about 6.0. There was no significant difference in pH between any of the particles solutions.

Figure 10 shows TEM images of unstabilized particles, particles synthesized with CMC, and particles synthesized with GA.

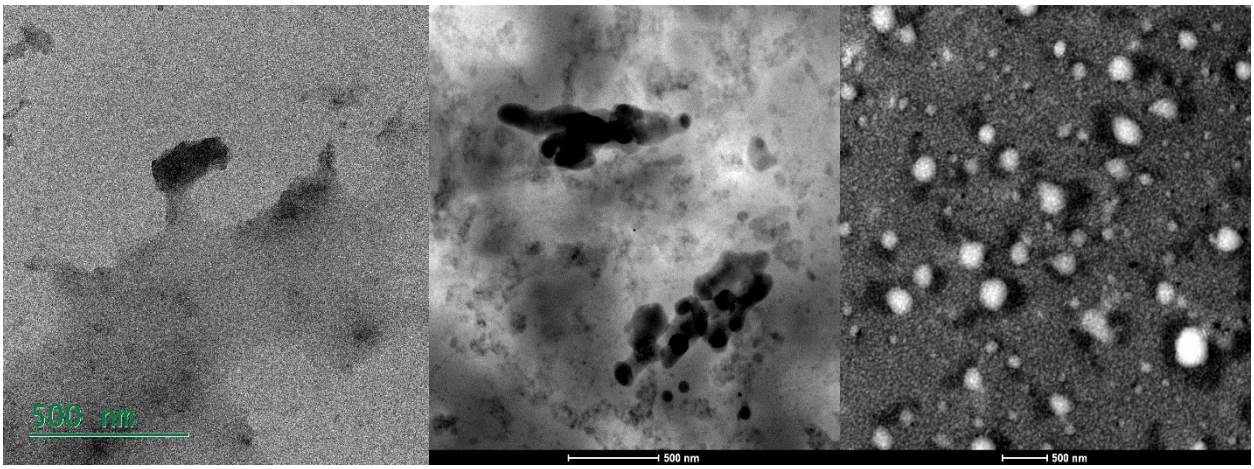

Unstabilized CMC Stabilized GA Stabilized

Figure 10: TEM images of unstabilized particles, particles synthesized with CMC, and particles synthesized with GA. The unstabilized particle image was taken in TEM mode, while the CMC and GA stabilized particle images were taken while the instrument was in scanning TEM mode.

The unstabilized particles appeared more agglomerated and non-uniform, while the particles synthesized with CMC and GA were more spherical and there were many more particles. The uneven background in all three images is due to compounds in the solution after synthesis. The GA particle solution had the most background interference, necessitating high contrast to visualize the particles.

2.3 Discussion

The widely variable size of particles synthesized with TA indicates that TA was not stabilizing the nZVI particles. The size of particles synthesized with PVP measured using DLS and NTA and the ZP was not significantly different than unstabilized particles, indicating PVP was not stabilizing the nZVI. The large HDD of unstabilized particles and particles synthesized with PVP soon after filtration through a 0.22 μm syringe filter indicates that these particles were agglomerating rapidly, and therefore not stabilized. This may be because the molecular weight of PVP is variable, and for a compound to function effectively as a stabilizer for nZVI it needs to have a high molecular weight or a large charge.

Particles synthesized with CMC and GA were under 200 nm when synthesized using both methods, which was significantly smaller than unstabilized particles demonstrating particle stabilization. These results suggest that the CMC and GA produce well-dispersed, small nZVI when used as a pre-synthesis stabilizer (Greenlee and Hooker, 2012). However, particle HDD measured with DLS increased when synthesis method 2 was used. This increase in size may be due to the difference in DLS instruments used. All size and ZP measurements made using the Brookhaven ZetaPALS instrument after synthesizing particles using method 1, while all HDD and ZP measurements of particles synthesized using method 2 were made using the Malvern Zetasizer instrument. The same NanoSight NS500 instrument was used for all NTA measurements, and when there are compared the second method resulted in smaller particles synthesized with GA and smaller standard error values. Therefore method 2 was chosen to synthesize particles for toxicity and reactivity tests.

The dissimilarity between NTA and DLS readings is due to the way the samples are analyzed. While NTA and DLS readings agree when the average particle diameter and polydispersity are low, they differ when larger particles are present which can obscure smaller particles in DLS measurements and bias size readings toward larger particles. NTA analyzes each particle individually, lessening the skew of the average HDD towards larger particles. The NTA software used produces a graph showing the particle size distribution in a sample, and the particles synthesized with CMC or GA had much smaller distributions than the unstabilized particles and those synthesized with PVP. This shows that the addition of the stabilizers is influencing the particle diameter, and keeping the particles from agglomerating.

The ZP values of particles synthesized with CMC and GA were significantly larger than unstabilized particles, indicating that these compounds were functioning as stabilizers. The ZP values of the stabilized particles were still above -30 mV, the limit of stabilization, which may be due to the low pH of the particle solutions. The pH of all three solutions was 1-2 below neutral, indicating excess hydrogen ions. These hydrogen ions may be due to the addition of sodium borohydride, which releases hydrogen when added to water. CMC molecules include carboxylic groups, which dissociate in solution and will contribute to lowered pH levels (He et. al, 2007). Additionally, the viscosity of GA has been found to decrease at pH values far from neutral, which is thought to be the result of the electrical double layer compressing (Islam et. al, 1997). This could affect the effectiveness of GA as a stabilizer by changing the electrostatic and physical properties of the nanoparticle dispersion. Each particle solution had a negative ZP value, so the positive hydrogen atoms will neutralize some of the negative charge surrounding each

particle. Neutralizing the pH of these solutions may lead to more stable dispersions (Malvern, 2015).

The particles synthesized with a stabilizing compound were smaller and more spherical based on TEM images. The particles synthesized with CMC and GA had much smaller HDD values than the unstabilized particles, suggesting that the agglomeration of the particles seen in the CMC image occurred during sample drying. The agglomerates appear to be connected by a different compound than what the particles are composed of, and this is thought to be CMC. The background interference seen in all three TEM images is probably caused by remaining compounds in the particle solution following synthesis, and may be ferrous sulfate, sodium borohydride, CMC, or GA.

Chapter 3 – Toxicity Testing

3.0 Introduction

The embryonic zebrafish (*Danio rerio)* model was selected as a model vertebrate system to investigate the toxicity of nZVI because the embryos are small, transparent, develop rapidly, and are more sensitive than adult zebrafish. These qualities allow studies to be conducted quickly and can provide insight into the toxicity of chemicals. Additionally, the molecular signaling, cellular structure, anatomy, and physiology of embryonic zebrafish are similar to other vertebrates including humans, making the embryonic zebrafish assay a useful tool to investigate the potential effects of exposure to nanoparticles (Harper et. al, 2011).

3.1 Embryonic Zebrafish Assay Materials and Methods

CMC stabilized, GA stabilized, and unstabilized nZVI dispersions were prepared using particle synthesis method 2 described in the above section to be used for toxicity testing. Particles were synthesized immediately prior to each toxicity test. Immediately following particle preparation, 1 mL of each nanoparticle solution was placed in a drying oven and weighed to determine the concentration of nanoparticles in each solution. All zebrafish embryos used in this study were obtained from the Sinnhuber Aquatic Research Laboratory at Oregon State University in Corvallis, Oregon. Both stabilized and unstabilized nZVI dispersions were prepared using serial dilution to concentrations of 10%, 20%, 30%, 40%, 50%, and 60% nanoparticle dispersion using embryo media just prior to exposure. Embryo media was prepared using water and Instant Ocean salts (Instant Ocean United Pet Group, Virginia, US), at a pH between 7.0 and 7.4. Embryo

media and stabilizer only controls were also used. When the embryos had reached the 6 hour post fertilization (hpf) developmental stage, the nanoparticle dispersions were vortexed for about 30 seconds and 150 microliters were placed in each well (n = 12 for each concentration) of two sterile 96 well plates. Two controls were used for each exposure: one with a stabilizer solution only and one with embryo media only. Embryos were exposed with the protective chorion intact to replicate environmental conditions and were incubated at 26 °C for five days under a 14:10 hour light:dark cycle. Embryos were observed at 24 hpf and were assessed for mortality, developmental progression, notochord malformations, and spontaneous movement abnormalities. At 120 hpf, the embryos were assessed for mortality, hatching, pericardial edema, the absence of circulation, yolk sac edema, body truncation, touch response, and other physical malformations. Mortality was determined by observing an embryo for at least 30 seconds while watching for a heartbeat. If no heartbeat was detected during the 30 seconds the embryo was recorded as deceased. All graphical error bars represent the standard error of the mean, calculated by dividing the standard deviation between the replicates by the square root of the number of replicates. All solutions were made immediately before exposure, and all syntheses and exposures were performed in triplicate. Student-t tests assuming equal variance were used to determine significant differences between all data.

3.2 Results

At 24 hpf, all embryos were unhatched, alive, and showed very few malformations. At 120 hpf, pericardial edema was present in some zebrafish, though mortality and hatch rate delays were the most prevalent abnormalities. The GA particle exposures exhibited less mortality than the unstabilized and CMC particle dispersions.

The unstabilized and CMC stabilized particles dispersions caused about equal mortality as shown in Figure 11.

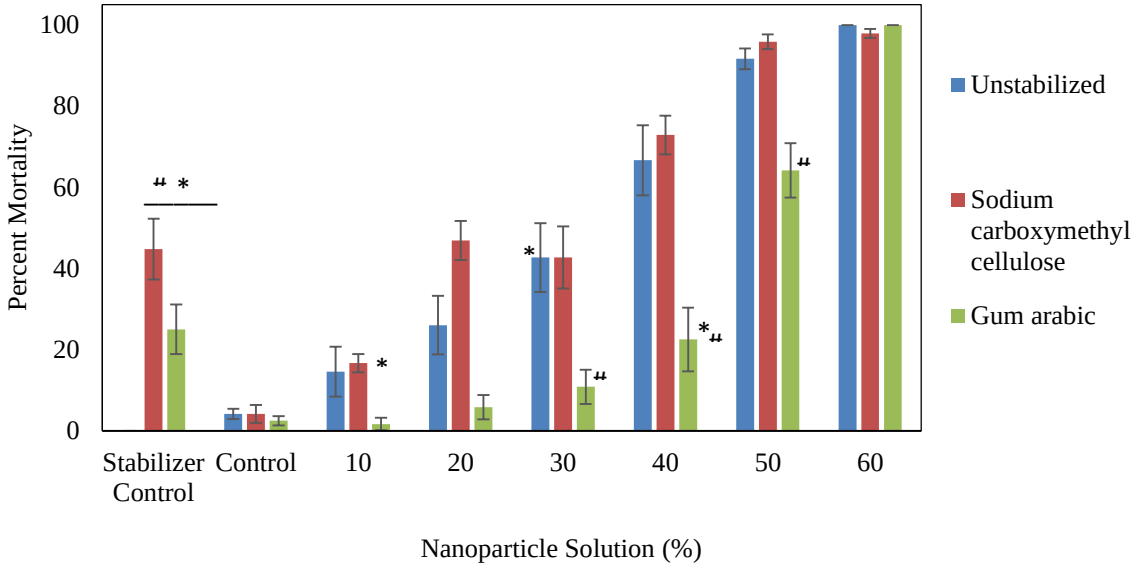

Figure 11: The percent of embryos that were dead 120 hours post fertilization following exposure to unstabilized particles or particles synthesized with CMC or GA for 114 hours shown with standard error bars. The lowest concentration that caused mortality significantly different from control is marked (* = P < 0.05), and all higher concentrations caused significant mortality. Significant difference from the other two treatments is marked (# = P < 0.05). GA stabilized particles caused significantly lower mortality than the CMC stabilized particles at all concentrations below 60%.

The CMC and GA stabilizer controls caused significant mortality at 0.8 wt% and 2.0 wt% respectively. The CMC control caused about 45% mortality and the GA caused about 25% mortality, and these values were significantly different from each other. Thirty percent unstabilized particle solution was the lowest concentration that caused significant mortality at about 14%, and the 10% CMC nanoparticle solution was the lowest that

caused significant mortality. The GA stabilized particles caused significant mortality at 40% nanoparticle solution, leading to about 64% mortality. The GA stabilized particles caused significantly less mortality than the particles synthesized with CMC at all concentrations below 60% nanoparticle solution, and significantly less mortality than the unstabilized particles at 30, 40, and 50% nanoparticle solutions. The unstabilized and CMC stabilized particles did not cause significantly different mortality at any concentration. Table 2 shows the concentrations in ppm that correspond to the nanoparticle solution percentages.

Particle Exposure Concentrations (mg/L)							
Stabilizer	**Stabilizer Control**	**10%**	**20%**	**30%**	**40%**	**50%**	**60%**
Unstabilized	N/A	713	1426	2139	2852	3565	4278
CMC	0.8 wt%	865	1730	2594	3459	4324	5189
GA	2.0 wt%	1455	2911	4366	5822	7277	8733

Table 2: The concentration of nZVI in each particle solution used for toxicity testing. The concentration of the GA stabilized particles was significantly higher than the other two.

The concentration of GA stabilized particles was significantly higher than the concentration of the CMC stabilized and unstabilized particles. The lethal concentration that killed 50% of the embryos (the LC50) was found to be 2480 ppm for unstabilized nZVI, 2922 ppm for CMC stabilized nZVI, and 7176 ppm for GA stabilized nZVI using linear interpolation of the mortality data.

Embryonic zebrafish hatch from the chorion at 72 hpf when kept in the conditions described in chapter 3.1, but many exposed embryos did not hatch at this time. The percentage of embryos that had not hatched 120 hpf is shown in Figure 12.

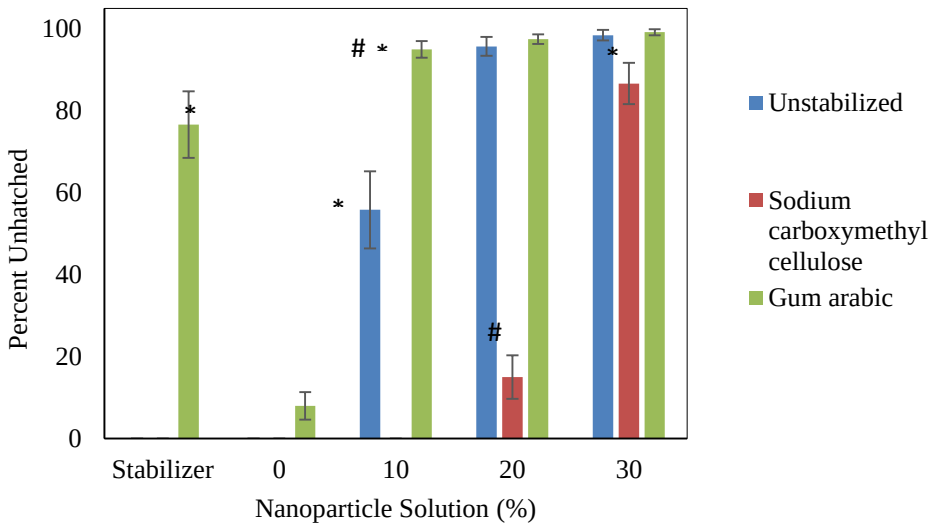

Figure 12: The percentage of embryos in each treatment unhatched at 120 hpf after nZVI exposure for 114 hours with standard error bars. The lowest concentration that caused hatching delay significantly different from control is marked, and all higher concentrations caused significant hatching delay. nZVI solutions that caused significantly different (# = $P < 0.05$) hatching delay than the other two treatments are also marked.

The GA control caused hatching delay in about 77% of embryos, which was significantly different from control, while the CMC control caused no hatching delay. Both the GA and unstabilized nZVI caused significant hatching delay at 10% nanoparticle solution. The GA and unstabilized nZVI caused hatching delay in 95 and 56% of the embryos respectively, but the GA nZVI caused significantly more hatching delay than the unstabilized and the CMC stabilized nZVI at this concentration. CMC nZVI caused about 15% hatching delay, which was significantly less than the unstabilized and GA stabilized particles at 20% nanoparticle solution which caused about 96 and 98% respectively. All three particle solutions caused significantly more hatching delay than control at 30% nanoparticle solution, and none were significantly different from each other. At this

concentration, the unstabilized particles caused 98% hatching delay, the CMC stabilized particles caused 87% hatching delay, and the GA stabilized particles caused 99% hatching delay.

Figure 13 shows representative images of embryos at 120 hpf exposed to 30% nanoparticle solutions.

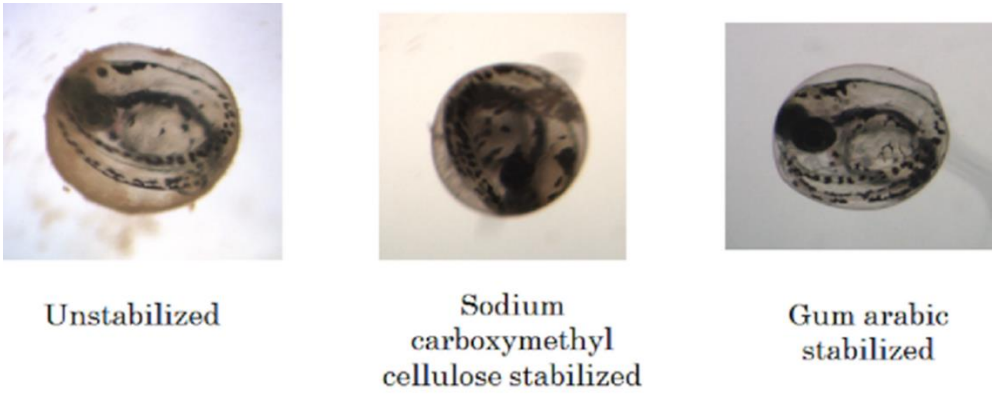

Figure 13: Embryotic zebrafish 120 hpf exposed to 30% a) unstabilized nZVI, b) CMC stabilized nZVI, or c) GA stabilized nZVI for 114 hours.

The chorion of embryos exposed to unstabilized nZVI became coated with iron oxide by the fifth day of exposure. The chorion of embryos exposed to GA stabilized nZVI became very tight around the embryo.

3.3 Discussion

The lower mortality of the GA stabilized particles despite the higher concentration suggests that the mortality caused by the CMC stabilizer control and stabilized particle dispersions was caused by the concentration of CMC used. The mortality caused by the unstabilized particle dispersions may have been due to generation

of reactive oxygen species produced by the reaction of iron with the oxygen in the exposure solutions (Chen *et al.*, 2013). The GA stabilized particles had the highest LC50, at 7176 ppm, indicating it caused the lowest mortality at higher concentrations than the other two dispersions. The GA stabilizer control and GA stabilized particle dispersions caused the most severe hatching delay. The chorion of embryos exposed to GA and GA stabilized particles became tight around the embryo, suggesting there may have been a higher concentration of salt in the GA solution than inside of the chorion, causing liquid to leave the chorion through osmosis. As the chorion shrunk around the embryos, their movement may have been restricted, making them less likely to break free of the chorion. Additionally, GA molecules may have attached to the outside of the chorion, leading to the delay in hatching. The embryo media control and CMC stabilizer control fish experienced no hatching delay, indicating that the GA concentration contributed to the hatching delay. The chorion of the embryos treated with unstabilized nZVI became coated with particle agglomerates (see Figure 13), which may have led to the delay in hatching and mortality by limiting oxygen flow to the embryo, slowing the breakdown of the chorion (Chen *et al.*, 2013). The small size of the GA stabilized particles and the high LC50 seen in these preliminary studies suggest that GA is an effective, less hazardous stabilizer for nZVI.

Chapter 4 – Reactivity Testing

4.0 Introduction

nZVI have been found to effectively degrade chlorinated organic solvents, including trichloroethylene (TCE). TCE is highly toxic contaminant used in vapor degreasing. Exposure to TCE can affect the central nervous system, and TCE is a suspected carcinogen. Human and animal exposure to TCE can result from TCE leaking into groundwater (EPA). TCE was chosen as a model organic contaminant to test the effect of stabilization on the ability of the particles to degrade contaminants. nZVI dechlorinate TCE through reduction, and can be modeled as a first order reaction (He et. al, 2007). Typically, hydrogen atoms displace the chlorine atoms, reducing TCE to dichloroethene (DCE), to vinyl chloride (VC), and finally to ethane as shown in Figure 14.

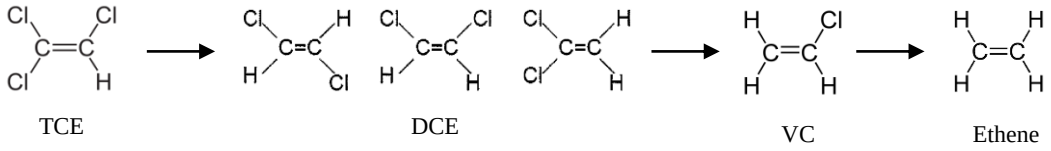

Figure 14: The typical reaction pathway of TCE to dichloroethene (DCE), vinyl chloride (VC), and finally ethene.

Both TCE and VC are considered priority pollutants by the United States Environmental Protection Agency (EPA). VC is a contaminant of concern like TCE because of its toxicity and carcinogenetic properties. Degradation of TCE can result in the accumulation of VC at contaminated sites (Liu, 2013). nZVI have been found to reduce TCE to ethane through an alternate route, shown below in Figure 15 (Xiu et. al, 2010).

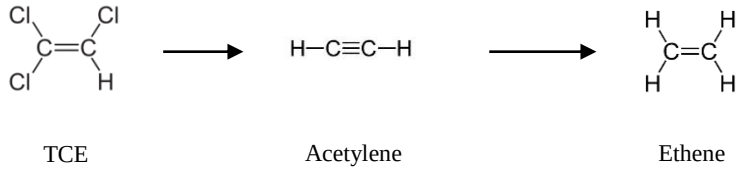

Figure 15: An alternate degradation pathway of TCE to ethane, caused by nZVI.

This pathway eliminates the production of VC and DCE, further reducing harmful contamination.

4.1 Reactivity Test Methods

All nanoparticle solutions were prepared immediately using particle synthesis method 2 prior to performing each reactivity test. Unstabilized, CMC stabilized, and GA stabilized particles were used for reactivity tests. Solutions with 6.25, 12.5, 25, and 50 ppm TCE were prepared using serial dilution to create a calibration curve. Initial incubations were carried out in 2 mL amber glass bottles with septum tops. A 0.5 mL aliquot was taken from the 50 ppm control and mixed with 0.5 mL of the nZVI dispersion. All solutions were placed on a shaker plate at 150 rpm for 24 hours. Immediately following incubation, the TCE content of each vial was determined using an HP 6890 series (Hewlett Packard, California, United States) gas chromatograph (GC) by injecting a sample of the headspace in each vial into the instrument. The GC used was equipped with a flame ionization detector, and had an oven temperature of 220 °C. The calibration curve was used to quantify TCE content in each sample. nZVI were synthesized immediately prior to each incubation. Student-t tests assuming equal variance

were used to determine significant differences between all data. All graphical error bars represent the standard error of the mean, calculated by dividing the standard deviation between the replicates by the square root of the number of replicates.

For later experiments, incubations were carried out in 125 mL clear glass Wheaton bottles with butyl septum tops. A 25 mL aliquot was taken from the 50 ppm control and mixed with 25 mL of the nZVI dispersion. The 125 mL bottles were also incubated for 24 hours on a shaker plate at 150 rpm, and the amount of TCE in the headspace after incubation was determined as described above.

4.2 Results

In trials performed using 2 mL amber glass vials, variable results were obtained. In some cases, the measured amount of TCE in the vial was greater than the concentration added. The results of incubation in 125 mL bottles is shown in Figure 16.

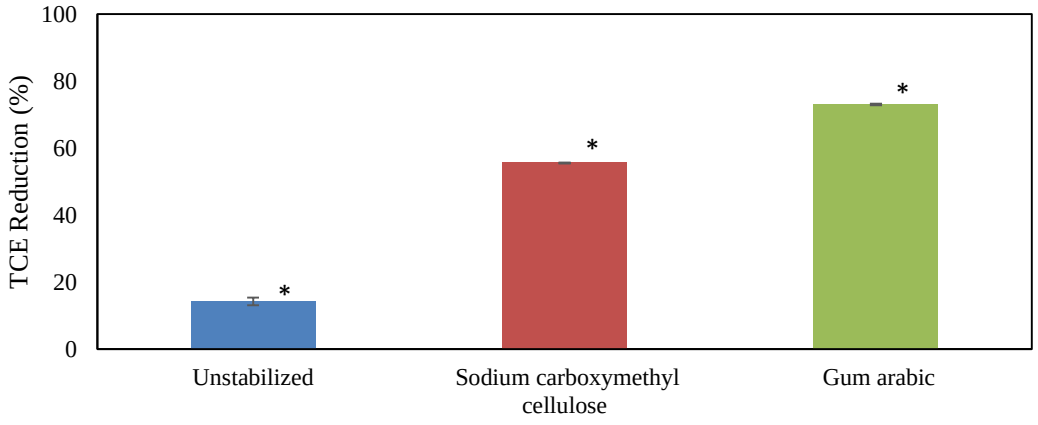

Figure 16: The percent reduction in 25 ppm TCE following 24 hour incubation with nZVI with standard deviation error bars. Unstabilized nZVI led to the least reduction in TCE, and GA stabilized particles led to the greatest. Each decrease was significantly different from the other two.

Unstabilized nZVI led to a 14% decrease, CMC stabilized particles led to a 56% reduction, and GA stabilized nZVI led to a 73% TCE decrease. Each of these results were significantly different from the others.

The surface area to volume ratio of each particle solution is shown in Table 3.

Stabilizer	Surface Area to Volume Ratio
Unstabilized	0.00367
CMC	0.02866
GA	0.04724

Table 3: The surface area to volume ratio of unstabilized nZVI, CMC stabilized nZVI, and GA stabilized nZVI. Each ratio was significantly different than the others.

The unstabilized particles had the lowest surface area to volume ratio, and the GA stabilized particles had the largest. Table 4 shows the concentration of nZVI incubated with TCE.

TCE Incubation Concentrations	
Stabilizer	**Concentration (mg/L)**
Unstabilized	3565
CMC	4324
GA	7277

Table 4: The concentration of nZVI incubated with each TCE sample for 24 hours. The concentration of GA stabilized particles was significantly higher than the other two.

The concentration of GA stabilized particles was significantly higher than the concentration of the other two samples.

4.3 Discussion

The trials performed in 2 mL vials were extremely variable; occasionally GC readings indicated that the concentration of TCE was greater than that added. This may have been due to the small headspace size. The space above the liquid was only 1 mL, and the composition in the headspace may have been inconsistent. Additionally, while on the shaker plate the liquid interactions with the vial walls may have prevented mixing and transport of TCE between the gas and liquid phases. Poor mixing may also have resulted in TCE moving into the headspace without every encountering nZVI, leading to very low degradation.

Preliminary experiments suggest the stabilized particles led to the largest reduction in TCE, with the GA stabilized particles reducing the concentration of TCE the most. Particles with larger surface area to volume ratios have more reactive sites available for reaction (Zhang et. al, 2014). The GA stabilized particles had the largest surface area to volume ratio suggesting that the larger ratio led to increased TCE reduction. Particles synthesized with GA had a larger concentration than particles synthesized with CMC and the unstabilized particles, so there were more particles available for reaction. However, the unstabilized and CMC stabilized particles did not have significantly different concentrations, and the CMC caused significantly more TCE reduction than the unstabilized particles. The surface area to volume ratio was the only parameter tested here that was significantly different for each treatment like the percent

TCE reduction, indicating that this was the property that led to the difference in reactivity.

Only one trial was run to obtain these results, and further trials are needed to determine if using the 125 mL bottles increases the accuracy of GC readings of TCE. Past studies have reported detecting 1, 1-DCE briefly during reactivity studies investigating the degradation of TCE using nZVI and no other degradation products (He et. al, 2007). No degradation products of TCE were detected in this study using the experimental setup described above, however further studies investigating the degradation products of TCE are recommended to determine if the TCE is transforming into DCE, VC, acetylene, or completely to ethene in the presence of nZVI. Additionally, nanomaterial reactivity has been found to be a strong function of pH, necessitating further investigation of the effect of pH on the reactivity of nZVI (He et. al, 2007).

Chapter 5 - Conclusions

The resulting solution and the efficacy and effects of using each stabilizer investigated in this work are summarized in Table 5.

Stabilizer	Resulting Materials	Efficacy	Effects
Unstabilized	Bare zero valent iron nanoparticles; larger particles that agglomerate quickly	Larger particles may move through soils less easily and will have less surface area available for reaction	Larger particles will not move through the groundwater as easily as smaller particles, resulting in less of an exposure risk to humans and animals; reduction of contaminants like TCE can result in toxic degradation products like VC
CMC	Stabilized zero valent iron nanoparticles and sodium carboxymethyl cellulose; small, well dispersed particles that are less likely to agglomerate than unstabilized particles	Smaller particles will move more easily through soils and will have larger surface area to volume ratios; carbon in the nanoparticle solution may act as a food source for microbes	Smaller particles will provide increased contaminant reduction, but will also move more easily through soils and may come into contact with humans and animals more readily than unstabilized particles; microbes may further degrade certain contaminants; reduction of contaminants like TCE can result in toxic degradation products like VC
GA	Stabilized zero valent iron nanoparticles and gum arabic; small, well dispersed particles that are less likely to agglomerate than unstabilized particles	Smaller particles will move more easily through soils and will have larger surface area to volume ratios	Smaller particles will provide increased contaminant reduction, but will also move more easily through soils and may come into contact with humans and animals more readily than unstabilized particles; reduction of contaminants like TCE can result in toxic degradation products like VC

Table 5: The resulting solution, efficacy, and effects of synthesizing unstabilized nZVI, and nZVI with CMC or GA.

The small size and larger ZP values compared to unstabilized particles indicates that the stabilizers tested here, CMC and GA, stabilized the nZVI when added during particle synthesis. Using the embryonic zebrafish model, the GA stabilized particles were found to cause the least mortality at the highest concentration when compared to CMC stabilized and unstabilized particles. The highest concentration of GA stabilized nZVI exposed here, 8733 ppm, may be higher than aquatic organisms would encounter after the particles have been diluted in groundwater. Investigation into the fate and transport of these engineered nanoparticles is also needed to determine the risk of exposure to both humans and animals.

Preliminary studies suggest adding a stabilizer during synthesis increases the efficacy of the particles, resulting in greater TCE degradation. The ability of the particles to degrade contaminants likely depends on the surface area to volume ratio of the particles. More work is needed to investigate the ability of GA stabilized nZVI to degrade contaminants in environmental conditions to better understand the remedial applications of these particles.

Integrating research on the efficacy and potential toxicity of nanomaterials used in environmental remediation can support sustainability goals and ultimately protect the environment from unforeseen impacts.

References

Appropriate Conditions of Oxidation By-Product Bromate Removal from Drinking Water by Nanoparticle Zero-Valent Iron: Journal of Environmental Engineering: (ASCE). (n.d.). Retrieved May 25, 2015, from http://ascelibrary.org.ezproxy.proxy.library.oregonstate.edu/doi/full/10.1061/%28ASCE%29EE.1943-7870.0000764

Bilardi, S., Calabrò, P. S., Caré, S., Moraci, N., & Noubactep, C. (2013). Improving the sustainability of granular iron/pumice systems for water treatment. *Journal of Environmental Management*, *121*, 133–141. http://doi.org/10.1016/j.jenvman.2013.02.042

Chen, P.-J., Wu, W.-L., & Wu, K. C.-W. (2013). The zerovalent iron nanoparticle causes higher developmental toxicity than its oxidation products in early life stages of medaka fish. *Water Research*, *47*(12), 3899–3909. http://doi.org/10.1016/j.watres.2012.12.043

Cundy, A. B., Hopkinson, L., & Whitby, R. L. D. (2008). Use of iron-based technologies in contaminated land and groundwater remediation: A review. *Science of The Total Environment*, *400*(1–3), 42–51. http://doi.org/10.1016/j.scitotenv.2008.07.002

Degradation of vinyl chloride (VC) by the sulfite/UV advanced reduction process (ARP): Effects of process variables and a kinetic model. (n.d.). Retrieved June 5, 2015, from http://www.sciencedirect.com.ezproxy.proxy.library.oregonstate.edu/science/article/pii/S0048969713003641

Dynamic light scattering for size characterization. (n.d.). Retrieved April 15, 2015, from http://www.malvern.com/en/products/technology/dynamic-light-scattering/

Greenlee, L. F., & Hooker, S. A. (2012). Development of stabilized zero valent iron nanoparticles. *Desalination and Water Treatment*, *37*(1-3), 114–121. http://doi.org/10.1080/19443994.2012.661262

Harper, S. L., Carriere, J. L., Miller, J. M., Hutchison, J. E., Maddux, B. L. S., & Tanguay, R. L. (2011). Systematic Evaluation of Nanomaterial Toxicity: Utility of Standardized Materials and Rapid Assays. *ACS Nano*, *5*(6), 4688–4697. http://doi.org/10.1021/nn200546k

He, F., & Zhao, D. (2007). Manipulating the Size and Dispersibility of Zerovalent Iron Nanoparticles by Use of Carboxymethyl Cellulose Stabilizers. *Environmental Science & Technology*, *41*(17), 6216–6221. http://doi.org/10.1021/es0705543

He, F., Zhao, D., Liu, J., & Roberts, C. B. (2007). Stabilization of Fe-Pd nanoparticles with sodium carboxymethyl cellulose for enhanced transport and dechlorination of trichloroethylene in soil and groundwater. *Industrial & Engineering Chemistry Research*, *46*(1), 29–34. http://doi.org/10.1021/ie0610896

Islam, A. M., Phillips, G. O., Sljivo, A., Snowden, M. J., & Williams, P. A. (1997). A review of recent developments on the regulatory, structural and functional aspects of gum arabic. *Food Hydrocolloids*, *11*(4), 493–505. http://doi.org/10.1016/S0268-005X(97)80048-3

Lin, S. (2012). Polymeric Coatings on Silver Nanoparticles Hinder Autoaggregation but Enhance Attachment to Uncoated Surfaces. *Langmuir*, *28*(9), 4178–4186. http://doi.org/10.1021/la202884f

Nutrition, C. for F. S. and A. (n.d.). Generally Recognized as Safe (GRAS) [WebContent]. Retrieved April 15, 2015, from http://www.fda.gov/Food/IngredientsPackagingLabeling/GRAS/

O'Carroll, D., Sleep, B., Krol, M., Boparai, H., & Kocur, C. (2013). Nanoscale zero valent iron and bimetallic particles for contaminated site remediation. *Advances in Water Resources*, *51*, 104–122. http://doi.org/10.1016/j.advwatres.2012.02.005

Sakulchaicharoen, N., O'Carroll, D. M., & Herrera, J. E. (2010). Enhanced stability and dechlorination activity of pre-synthesis stabilized nanoscale FePd particles. *Journal of Contaminant Hydrology*, *118*(3–4), 117–127. http://doi.org/10.1016/j.jconhyd.2010.09.004

US EPA, O. (n.d.). Trichloroethylene | Technology Transfer Network Air Toxics Web site | US EPA. Retrieved April 15, 2015, from http://www.epa.gov/airtoxics/hlthef/tri-ethy.html

Xiu, Zong-ming, Zhao-hui Jin, Tie-long Li, Shaily Mahendra, Gregory V. Lowry, and Pedro J. J. Alvarez. "Effects of Nano-Scale Zero-Valent Iron Particles on a Mixed Culture Dechlorinating Trichloroethylene." *Bioresource Technology* 101, no. 4 (February 2010): 1141–46. doi:10.1016/j.biortech.2009.09.057.

Yang, R. S. H., & Rauckman, E. J. (1987). Toxicological studies of chemical mixtures of environmental concern at the National Toxicology Program: Health effects of groundwater contaminants. *Toxicology*, *47*(1–2), 15–34. http://doi.org/10.1016/0300-483X(87)90158-2